arXiv:1608.05680v1 [nucl-th] 19 Aug 2016

Formation of hypernuclei in heavy-ion collisions around the threshold energies.

A.S. Botvina[1,2], K.K. Gudima[1,3], J. Steinheimer[1], M. Bleicher[1], J. Pochodzalla[4]

[1]*Frankfurt Institute for Advanced Studies and ITP J.W. Goethe University, D-60438 Frankfurt am Main, Germany*

[2]*Institute for Nuclear Research, Russian Academy of Sciences, 117312 Moscow, Russia*

[3]*Institute of Applied Physics, Academy of Sciences of Moldova, MD-2028 Kishinev, Moldova and*

[4] *Helmholtz-Institut Mainz and Institut für Kernphysik, J.Gutenberg-Universität Mainz, D-55099 Germany*

(Dated: August 22, 2016)

Abstract

In relativistic ion collisions there are excellent opportunities to produce and investigate hypernuclei. We have systematically studied the formation of hypernuclear spectator residues in peripheral heavy-ion collisions with the transport DCM and UrQMD models. The hyperon capture was calculated within the potential and coalescence approaches. We demonstrate that even at the beam energies around and lower than the threshold for producing Λ hyperons in binary nucleon-nucleon interactions a considerable amount of hypernuclei, including multi-strange ones, can be produced. This is important for preparation of new experiments on hypernuclei in the wide energy range. The uncertainties of the predictions are investigated within the models, and the comparison with the strangeness production measured in experiments is also performed.

PACS numbers: 25.75.-q , 21.80.+a , 25.70.Mn

I. INTRODUCTION

In nuclear reactions the detailed studies of the three-flavor processes, including u, d and s quarks, will be mandatory to develop fundamental nuclear theories of hadrons and nuclei, as well as the large spectacular cosmic objects like neutron stars. Having a core with supra-nuclear densities and a crust with sub-nuclear densities, these stellar objects merge all aspects of nuclear physics. Baryons with strangeness embedded in the nuclear environment, i.e., hypernuclei, are the only available tool to approach the many-body aspect of the strong interaction at low energies. Hypernuclei are formed when hyperons ($Y = \Lambda, \Sigma, \Xi, \Omega$) produced in high-energy interactions are captured by nuclei. They live significantly longer than the typical reaction times, therefore, they can serve as a tool to study the hyperon–nucleon and hyperon–hyperon interactions. The investigation of hypernuclei is a very progressing field of nuclear physics, since it provides complementary methods to improve traditional nuclear methods and open new horizons for studying particle physics and nuclear astrophysics (see, e.g., [1–8] and references therein).

Recently very encouraging results on hypernuclei come from experiments with relativistic ion collisions. Many experimental collaborations (e.g., STAR at RHIC [9]; ALICE at LHC [10]; PANDA [11], FOPI, HADES, CBM [12, 13], and HypHI, Super-FRS, R3B at FAIR [14–16]; BM@N and MPD at NICA [17]) have started or plan to investigate hypernuclei and their properties in reactions induced by relativistic hadrons and ions. The limits in isospin space, unstable nuclear states, multiple strange nuclei and precision lifetime measurements are unique topics of these fragmentation reactions.

It is important in this respect to note that the very first experimental observation of a hypernucleus was obtained in the 1950-s in reactions of nuclear multifragmentation induced by cosmic rays [18]. Recently a remarkable progress was made in investigation of the multifragmentation reactions associated with relativistic heavy-ion collisions (see, e.g., [19–22] and references therein). This gives us an opportunity to apply well known theoretical methods adopted for description of these reactions also for production of hypernuclei [23, 24].

Specially, we emphasize a possibility to form hypernuclei in the fragmentation processes in peripheral collisions. The insight into mechanisms of such processes will provide access to the EoS of hyper-nuclear matter and explain the phase transition phenomena at low temperature. As already discussed [7, 25] in these reactions one can get a very broad

distribution of produced hypernuclei including the exotic ones and with extreme isospin. This can help to investigate the structure of nuclei by extending the nuclear chart into the strangeness sector [1–4]. In addition, complex multi-hypernuclear systems incorporating more than two hyperons can be created in such energetic nucleus-nucleus collisions, and this may be the only conceivable method to go even beyond $|s|$=2.

It was demonstrated in the previous works [26, 27] that the yields of single hypernuclei originating from the spectator residues in peripheral ion collisions will saturate with energies above 3–5 A GeV (in the laboratory frame). Therefore, the accelerators of moderate relativistic energies can be used for the intensive studies of hypernuclei. The subthreshold production of hyperons becomes possible in these reactions down to the energies of ∼1 A GeV. At the laboratory energies of ions around 1–2 A GeV the detection of hypernuclei can become very effective and this give an advantage despite of their smaller yields in comparison with high energy beams. For example, the novel experimental set-ups, like FRS/Super-FRS [16, 28, 29], can be effectively used for separation of nuclei with energies less than 2 A GeV, that essentially extends opportunities for their investigation. This gives chances to measure many new exotic hypernuclei. The acceptance of other modern detectors, like CBM at GSI/FAIR [13] or STAR at RHIC [9] allows to register particles coming mostly from the kinematic region around midrapidity. Therefore, the decreasing of the beam energy will increase considerably the probability for fragments produced in the target/projectile region to enter the detection domain. Since the formation of large hypernuclei is shifted toward the target/projectile rapidities [27], this can open possibilities to form novel hypernuclear states. Another research direction is related to producing multi-strange hyper-fragments which may require a higher beam energy. This needs a systematic theoretical investigation of double- and multi-strange fragment yields at least at beam energies up to ∼10 A GeV in order to understand if any saturation phenomenon can be observed. The light multi-strange clusters can be measured with the high precision detectors, for example, by CBM collaboration [13]. The aim of this theoretical work is to investigate the hypernuclei production in detail the region of the beam energies of 1–10 A GeV, including the comparison with available experiments and the parameter dependence of the results, in order to provide the future experiments with reliable predictions of these reactions.

II. MODELS FOR PRODUCTION OF HYPERNUCLEI AT RELATIVISTIC COLLISIONS

We recall shortly the mechanisms for producing hypernuclei which were discussed previously: The formation processes of hypernuclei are apparently different in central and peripheral ion collisions. There are indications that in central collisions of very high energy the coalescence mechanism, which assembles light hyper-fragments from the produced hyperons and nucleons (including anti-baryons), is essential [9, 10, 30, 31]. Thermal models suggest also that only the lightest clusters, with mass numbers $A \lesssim 4$, can be noticeably produced in this way because of the very high temperature of the fireball (T≈160 MeV) [32, 33]. On the other hand, it was claimed long ago that the absorption of hyperons in the spectator regions after peripheral nuclear collisions is a promising way to produce hypernuclei [25, 34–36]. The special reactions associated with these processes, e.g., the hyper-fission, were under investigation too [37, 38]. An important feature of peripheral collisions is that large pieces of nuclear matter around normal nuclear density at low temperature can be created in contrast to the highly-excited nuclear matter at mid-rapidity. Nucleons from the overlapping parts of the projectile and target (participant zone) interact strongly among themselves and with other hadrons produced in primary and secondary collisions. Nucleons from the non-overlapping parts do not interact intensively, and they form residual nuclear systems, which we call spectator residues. We remind that these residues are formed during first 30–60 fm/c after starting the collision, when energetic hadron-nucleon interactions inside nuclei cease and the remaining nucleons do not escape the nucleus potential [19, 25]. The nuclear system evolves toward thermalization in this case. It is well established that low excited spectator residues ($T \lesssim$ 5-6 MeV) are produced in such reactions [19–21, 39]. The production of hyperons is associated with nucleon-nucleon collisions, e.g., $p+n \rightarrow n+\Lambda+K^+$, or collisions of secondary mesons with nucleons, e.g., $\pi^+ + n \rightarrow \Lambda + K^+$. Strange particles may be produced in the participant zone, however, the particles can re-scatter and undergo secondary interactions. As a result the produced hyperons populate the whole momentum space around the colliding nuclei, including the vicinity of nuclear spectators, and can be captured by the spectator residues. General regularities of the decay of such hyper-residues into hyper-fragments can be investigated with statistical models (e.g., generalized Statistical Multifragmentation Model SMM [23, 24]), which were previously applied for description of

normal fragments in similar processes with great success [19–22].

The theoretical predictions of strangeness and hyperon production in hadron and ion reactions can be performed with various dynamical models employing similar general assumptions on the hadron transport in nuclei but with different methods of solution of the kinetic equations. In addition, the models can also be different (especially at high energy) in the description of elementary hadron-hadron interactions and production of new particles. Previously we have investigated the model-dependence of the results [25, 27]. At relatively low-energy elementary hadron collisions (less than 1–3 GeV in the laboratory frame) the models use usually some approximations for the reaction channels supported by the analysis of available experimental data. However, at higher energies, where hyperon formation probability is large, theoretical evaluations are mostly used. For example, the Dubna Cascade Model (DCM) [25, 26, 40] involves the quark gluon string model (QGSM). The Ultrarelativistic Quantum Molecular Dynamics (UrQMD) model [41, 42] has adopted the string formation and its fragmentation according to the PYTHIA model for hard collisions. In particular, the current versions of DCM and UrQMD include up to 70 baryonic species (including their anti-particles), as well as up to 40 different mesonic species, which are involved in binary interactions. The Lund FRITIOF string model (including PYTHIA) is used in the Hadron String Dynamics model (HSD) [43], however, for simulations including in-medium self-energies of particles. We have shown that at high energy the difference between these models have a moderate influence (within the factor of two) on the yield of hypernuclei, that can be considered as an uncertainty of their prediction [27]. The capture of produced Λ hyperons by nuclear spectator residues can be easily obtained within the potential criterion [25]: It takes place if a hyperon kinetic energy in the rest frame of the residue is lower than the attractive potential energy generated by neighbouring nucleons, i.e., the hyperon potential, which is around 30 MeV in matter at normal nuclear density $\rho_0 \approx 0.15 fm^{-3}$. The variation (mostly, decreasing) of the nuclear density is taken into account during the hadron cascade development in nuclei and the hyperon capture potential varies correspondently [25]. The coalescence criterion [33], which uses the proximity of baryons in momentum and coordinate space, is consistent with the potential one. A generalization of the coalescence model [27], the coalescence of baryons (CB), can be applied after the dynamical stage described, for example, by DCM, UrQMD, and HSD models. In such a way it is possible to form primary fragments of all sizes, from the lightest nuclei to the heavy residues, including

hypernuclei within the same mechanism. We have found previously [27] that the optimal time for applying the coalescence (as the final state interaction) is around 40–50 fm/c after starting the heavy-ion collisions, when the rate of individual inelastic hadron interactions decreases very rapidly. A variation of the time within this interval leads to an uncertainty in the yield around 10% for a fixed coalescence parameter. This is essentially smaller than the uncertainty in the coalescence parameter itself. It is important that the calculations are performed on the event-by-event basis, like the experimental data are obtained. The following break-up of excited primary fragments can be described with the statistical models [23, 26, 44] by using the same Monte-Carlo method, which allows to keep information on each produced particle. The advantage of this hybrid procedure is the possibility to predict the correlations of yields of hypernuclei, including their sizes, with the rapidity, and with other produced particles.

In this paper we concentrate on the transport approaches and the capture of Λ hyperons. In particular, we show new systematic calculations with DCM and UrQMD models for various target/projectiles at relevant energies, as well as the comparison with available experimental data on strangeness production. We demonstrate also the sensitivity of the hyper-fragment yields to the parametrization of the hyperon production and its capture. We believe that in this way one can realistically estimate the primary hyper-fragments yields that is important for the planning of future experiments.

III. FORMATION OF HYPERONS AND STRANGE PARTICLES

The transport models were used successfully for description of strangeness production (see, e.g., Refs. [25, 45–47]). However, there are only few experimental data concerning the hyperon production. Some of them were analyzed in the previous works [25]. In Fig. 1 we show the comparison of DCM with the Λ-hyperon rapidity distributions measured by FOPI (GSI) collaboration for central and semi-central events (the estimated impact parameters are less than 5.5 fm). One can see a rather good agreement, which was obtained when the processes involving secondary interactions of produced particles were included [25, 35]. In the rapidity region of the projectile/spectators, one can note a slight surplus of the hyperons in the calculations. This should be tested with future measurements when the experimental efficiency will be improved at these rapidities.

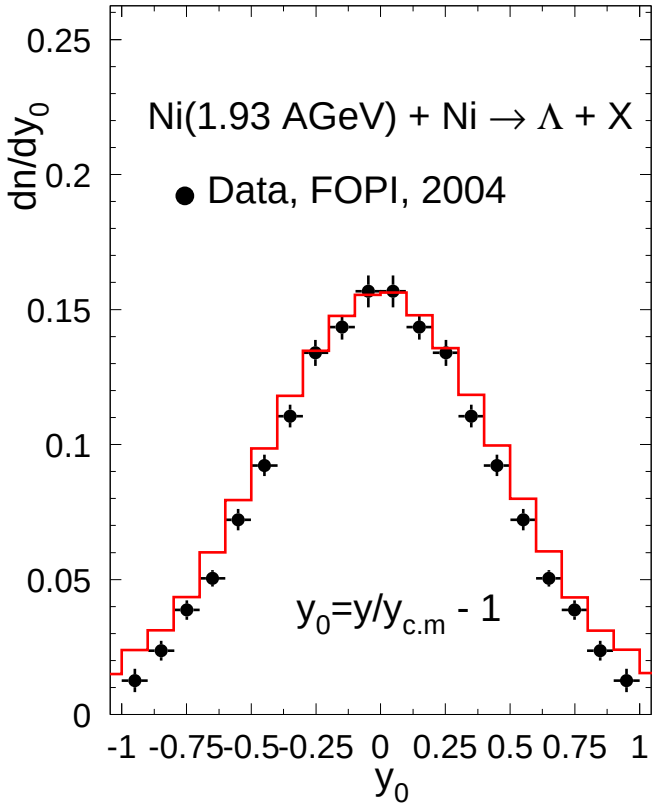

FIG. 1: (Color online) Rapidity distribution of Λ hyperons as measured by FOPI collaboration [48] in comparison with DCM calculations. The Ni + Ni reaction at 1.93 A GeV is analyzed for central and semi-central events.

The above projectile energy is still larger than the threshold for Λ production in the nucleon-nucleon collision ($E_{thr} \approx 1.6$ A GeV). On the other hand the subthreshold production is possible, because of the Fermi motion of nucleons in colliding nuclei and secondary rescattering processes. In order to verify the calculations at energies lower than E_{thr} we could look at the reaction products which accompany the hyperon production in this case. In particular, the channels with the K^+ formation, are dominating here. Therefore, in Fig. 2 and Fig. 3 we analyze the yields of positive kaons at the subthreshold energies. One see a quite reasonable agreement of the DCM transport calculations with the KAOS experimental data on the differential spectra at various angles. We should take into account that namely these spectra are used for the final fit and evaluation of the total kaon yields in the

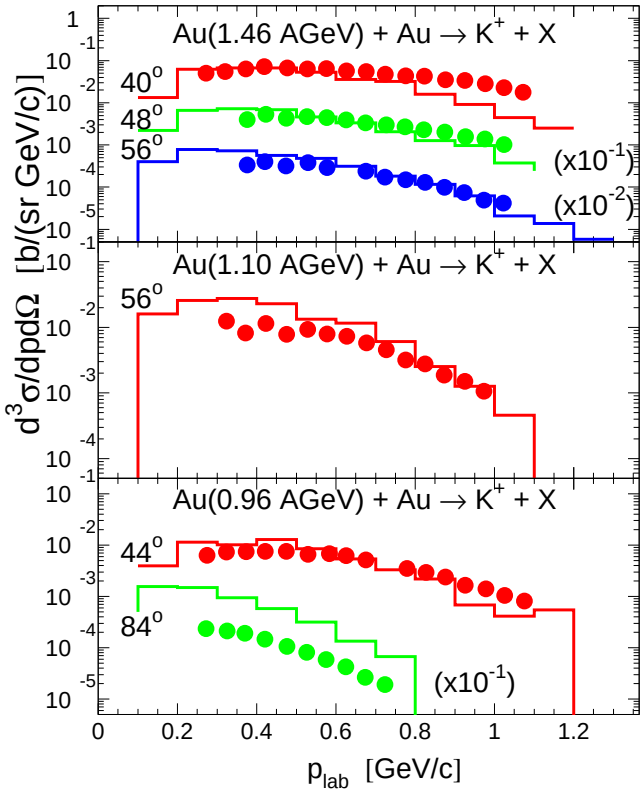

FIG. 2: (Color online) Double differential cross sections as functions of the laboratory particle momenta for the production of K^+ mesons in the gold-on-gold collisions at subthreshold energies under different angles. The experimental data (solid circles) are taken from Ref. [49]. The DCM calculations (solid histograms) are integrated over all impact parameters to meet the experimental conditions. The energies and angles in the laboratory system are given in the panels. The scaling factors are given in the brackets.

experiments. One can see a slight overestimation of the kaon production in the model under large angles (in the backward direction). However, they are responsible for a small part of the yield. Unfortunately, it was not possible to detect kaons with very low momenta and this leads to an uncertainty in the estimate of the total yield. However, we believe that within the model we can give a reasonable evaluation of the strangeness production in the subthreshold region. It is sufficient for the preparation of experiments on strange particles and fragments, if one can detect such particles (via products of their decay) with the cross

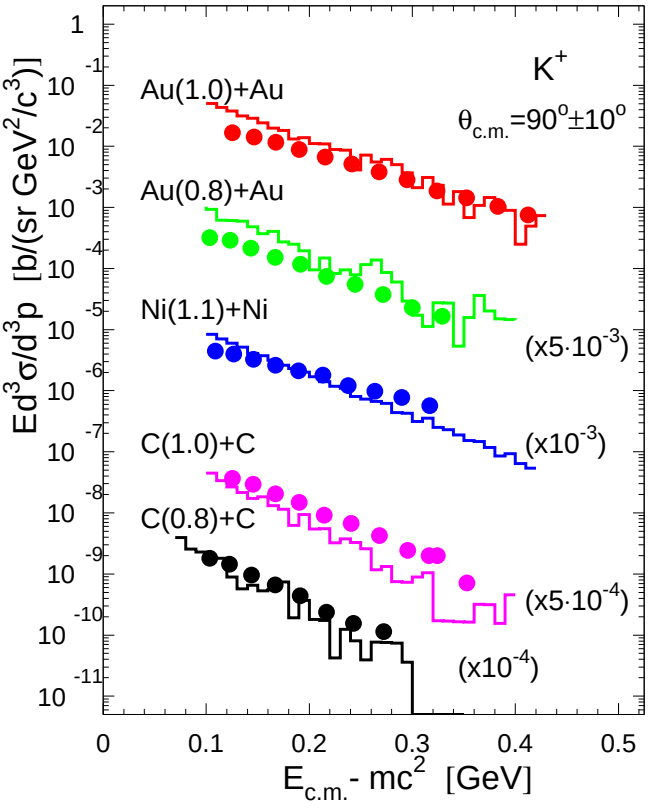

FIG. 3: (Color online) Invariant cross sections for the production of K^+ mesons in the center-of-mass system versus their kinetic energy under the angle of 90 degree, in the gold, nickel and carbon symmetric ion collisions. The experimental data (solid symbols) are taken from Ref. [50]. The DCM calculations are given by histograms. The energies in the laboratory system (in A GeV) and the scaling factors are shown in the panels.

sections of around nanobarns.

If we analyze the laboratory energies around and above the threshold, then the model predictions reproduce the experimental data better. This can be seen from Figs. 4 and 5. An underestimation of the positive kaons of high energy with DCM (Fig. 4) should have a minor effect, and it is just indicating that the number of Λ hyperons, which accompany the kaons, may be even larger. Though at this energy range the kaons were under selective study with other transport models (for example, see [45, 46] and references therein) the mechanism of their formation is still under discussion. We believe that the available direct

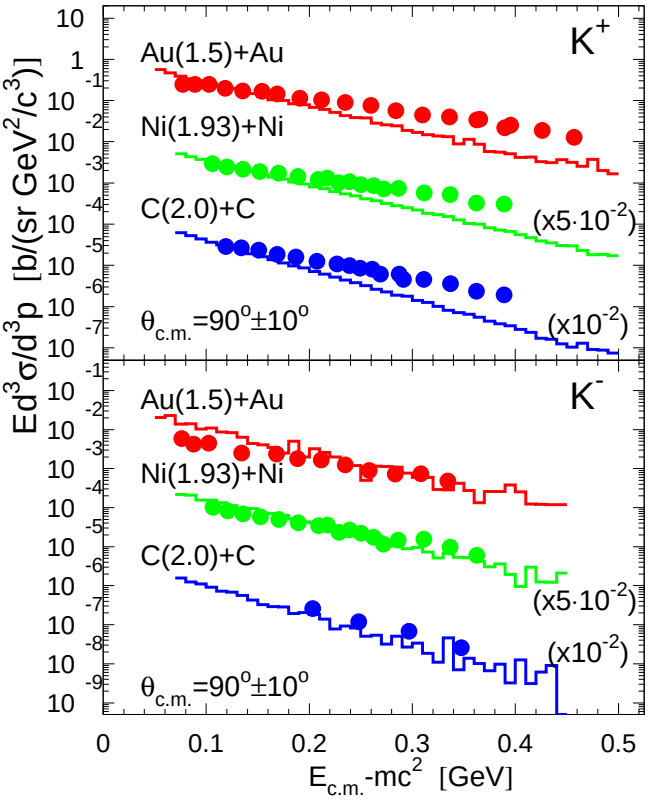

FIG. 4: (Color online) The same as in Fig. 3, however, in the collisions at higher energies, and for K^+ and K^- mesons (top and bottom panels).

hyperon distributions, shown here in Fig. 1 and in Ref. [25], should be analyzed within other models too. As seen from our analysis all kaon spectra can be reasonably described within DCM transport approach and this is a good justification for extending the model predictions to other strange particles. In our opinion it would be useful to perform a cross-comparison of different models on strangeness production around the threshold energy for clarifying the physics behind. Having in mind that controlling verifications of the transport codes are still necessary, we think we can afford a reasonable estimate of the hyper-fragment yields with the determination of the yield uncertainty also. In this case the effect of the hyperon capture by nucleons and clusters can be evaluated with help of additional model parameters.

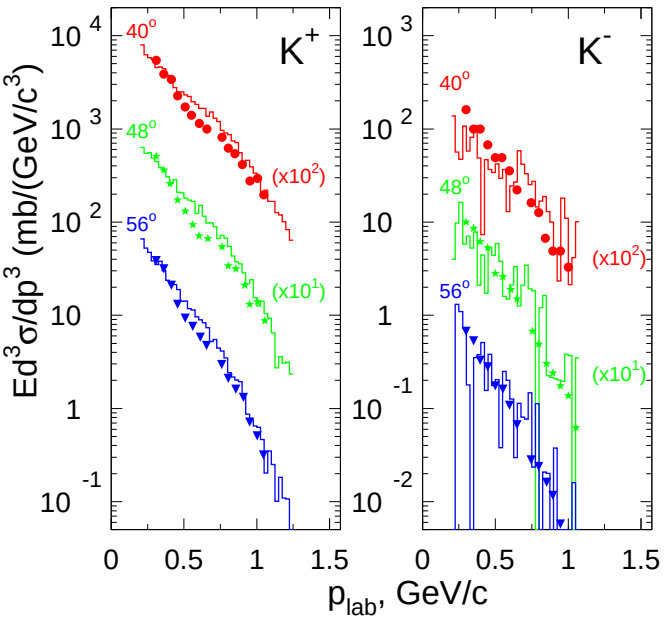

FIG. 5: (Color online) Invariant cross sections for the production of K^+ and K^- mesons in reactions induced by protons with the energies of 3.5 GeV on the gold target versus their momenta under several angles. All values are in the laboratory system, see notations on the panels. The symbols are experimental data taken from Ref. [51], the DCM calculations are histograms.

IV. PRODUCTION OF HYPER-RESIDUES

It was discussed that the hyperon capture can be described by both the potential and the coalescence approach [25, 27]. The coalescence is very popular and it exists on the market in different modifications, see, for example, its application for the hyperon capture within other transport approaches [36, 52, 53]. The connection of the potential and coalescence capture conceptions was demonstrated previously. In particular, the momentum distribution of the hyperon captured in the nuclear potential well reminds a step-like function, see Fig. 10 in Ref. [25]. This can be approximated with the coalescent capture of hyperons if their momenta (or velocities) relative to other nucleons less than a certain value. It is important to compare the capture probability within the two approaches. Our understanding is that this capture is a fast process, which happens during the time around few tens fm/c from the beginning of the reaction. As a result, the most produced hyper-clusters should be excited

from low excitations up to few MeV per nucleons. They will decay afterwards during a very prolonged time ($\sim 10^2 - 10^4$ fm/c). It is well known that the secondary decay involves many-particle correlations which are usually not included in transport models. Such decay processes were already under examination [7, 23, 44] with the statistical models. We plan to pursue it in the forthcoming papers because these processes are universal and can take place not only in ion reactions. Below we demonstrate in detail the results concerning the hot primary hyper-residues' production, obtained within DCM and UrQMD+CB approaches.

In Figs. 6, 7, and 8 we show the yields of spectator residues after the capture of 1, 2, and 3 Λ hyperons. The collisions of light, medium, and heavy nuclei were considered in the large range of the projectile energies. The DCM calculations were performed with the potential capture criterion. The yields are presented in millibarns for the future convenient comparisons with experiments. Some curves are scaled with the factors shown in brackets on the figures. As was previously reported there is a trend of the yield's saturation at high energy [26]. The present calculations with large statistics demonstrate that this saturation trend can be still partly valid for double and even triple hyper-residues if the energy is well above the threshold. This confirms that the energies of $\sim$10 A GeV are already sufficient for producing multi-strange hypernuclei. We have also investigated the influence of the hyperon capture potential on the hyper-fragment formation. Its formal decreasing from 30 to 15 MeV (for normal nuclear matter), which we consider as a maximum reasonable variation, leads to decreasing the hyper-residue yields by around 20% only. The reason is that the hyperon–nucleon cross-section increases very much at low energy, as assumed in the parametrization adopted in Ref. [25]. Since the nuclear matter is moderately diluted after the cascade of first fast particles the low-energy interactions with remaining nucleons become more probable. Therefore, as a result of these secondary interactions the Λ hyperon energy decreases very fastly in this energy domain and this looks as thermalization.

The production of hypernuclei around the threshold energy is instructive since it is sensitive to the properties of particles inside the nuclear matter of colliding nuclei, including the nucleon correlations. It is also practical since it can facilitate the experimental identification of hypernuclei, as we have mentioned in Introduction. To verify the predictions of the transport approaches at these energies we have also performed UrQMD calculations with a large statistics for lead on lead collisions at the energies of 1, 1.5 and 2.0 A GeV. With this model we can use the coalescence capture criterion and estimate the influence

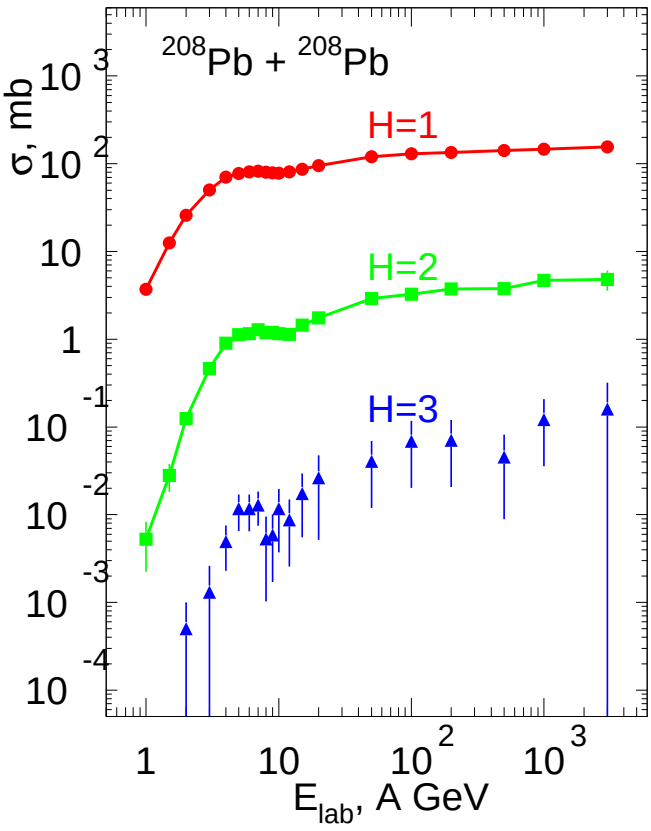

FIG. 6: (Color online) Absolute yields (in mb) of the hyper-spectator residues (projectiles or targets) in lead on lead collisions versus the laboratory energies. The numbers of captured Λ hyperons (H) are shown in the figure. The statistical variances ('error bars') of the performed DCM calculations are shown if they are larger than the size of the symbols.

of various coalescence parameters. The procedure was described in detail in our previous work [27] and concerns both the relative coordinates and velocities between the coalescent nucleons. In particular, the velocity coalescence parameter $v_c \approx 0.1$ should correspond to the formation of lightest clusters in the ground states. While the parameter $v_c \approx 0.22$, encloses the nucleons with velocities close to the Fermi motion in nuclei. This large parameter is also consistent with the momenta of hyperons absorbed by big spectators [25], therefore, it should be more realistic to describe the formation of larger nuclei which are expected for the target and projectile residues.

As a result, the UrQMD+CB calculations for $v_c = 0.22$ predict the following cross-sections

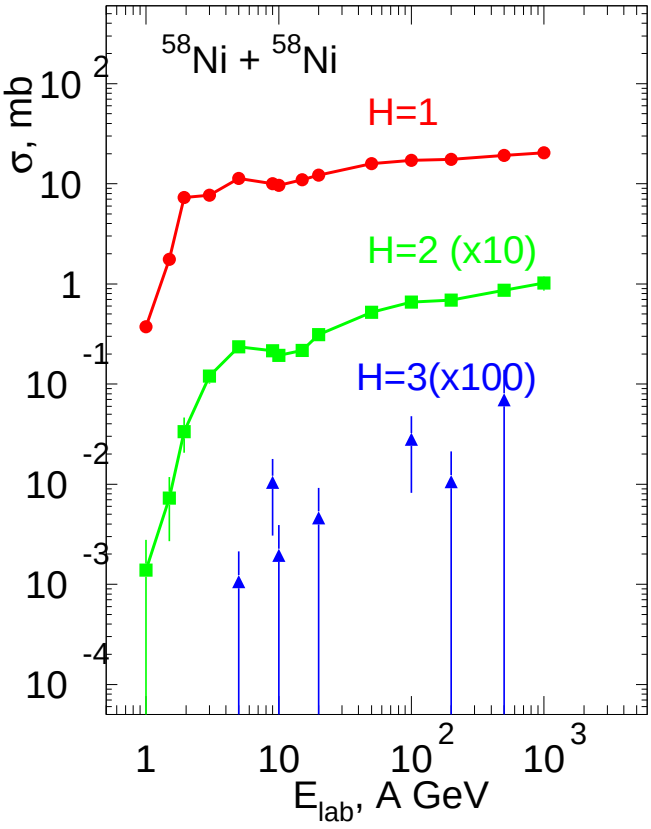

FIG. 7: (Color online) Absolute yields (in mb) of the hyper-spectator residues (projectiles or targets) in nickel on nickel collisions. The notations are as in Fig. 6, besides the scaling factors given in the brackets.

for producing the single hyper-residues: 0.35 mb at 1 A GeV, 2.4 mb at 1.5 A GeV, and 9.0 mb at 2 A GeV. By comparing it with the DCM presented in the fig. 6, one can evaluate the difference between DCM and UrQMD results. The artificial reducing of v_c to 0.1 leads to decreasing the yields to 0.1 mb, 0.75 mb, and 2.6 mb, respectively. However, it is a clearly underestimated case since such small parameters are typical for lightest clusters ($A \lesssim 4$), not for heavy residues. For the capture of two hyperons by the spectator residues in the more realistic $v_c = 0.22$ case we have got the following cross sections: 0.0013 mb, 0.011 mb and 0.045 mb for 1.0, 1.5 and 2.0 A GeV, correspondently. One can say that various models may lead to the deviations of up to one order at the very low subthreshold beam energy (1 A GeV), and the difference becomes smaller, approximately the factor two-three, at 2 A GeV.

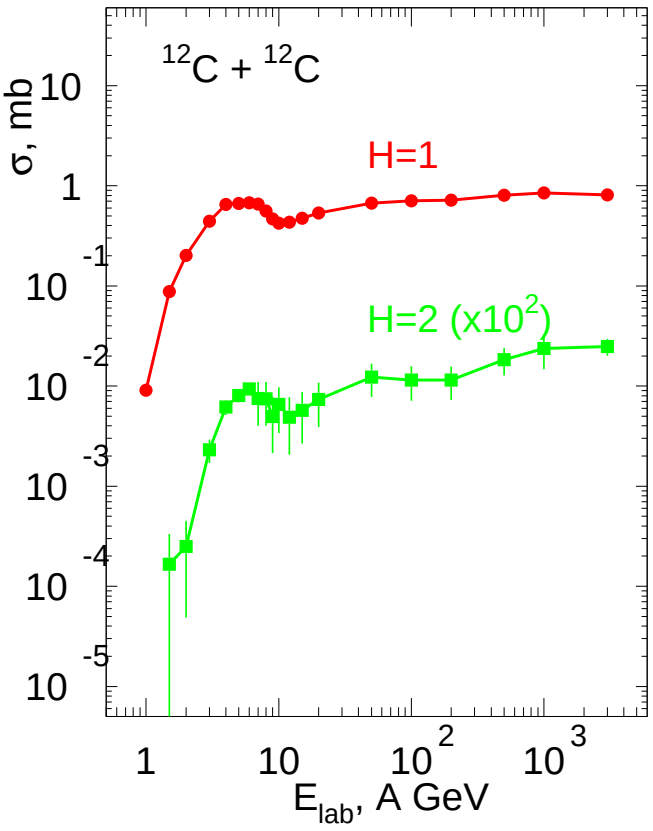

FIG. 8: (Color online) Absolute yields (in mb) of the hyper-spectator residues (projectiles or targets) in carbon on carbon collisions. The notations are as in Figs. 6, 7.

At high energy, as was discussed in the previous works [25, 27], the deviations in predictions of transport models are not more than the factor two.

We have analyzed that by increasing the coalescence parameters one may try to simulate the effect of the spectator nucleon density fluctuations within the coalescence picture and increase the capture effectively. However, the main discrepancy between the models comes from the difference in the hyperon production: The yield of hyperons integrated over all impact parameters in DCM is nearly 4 times larger than in UrQMD for Pb + Pb collisions at 1 A GeV. This discrepancy comes from the different parametrizations for strangeness production and particle rescattering at low energy. It depends also on the effective masses and potentials of particles in medium. The Fermi motion of nucleons may allow for high momentum components, that is very important in subthreshold reactions. All these phe-

nomena, which are not very crucial at very high energy, are treated in the models in different ways. The lack of the experimental data on low energy particles in subthreshold heavy-ion collisions is the main obstacle for the adequate adjustment of the models. However, we think that the presented results on the production of hypernuclei in the subthreshold region is a reasonable guide-line for their future experimental studies. Moreover, we believe that the experimental determination of the yields of spectator heavy hypernuclei, for example, by measuring remnants of the hyper-fission, may provide additional opportunities for the better description of the strangeness mechanisms inside nuclear matter at such low energies. This can also put the important constraint on interaction of hyperons in medium, since slow hyperons can be captured by the residues.

It is especially instructive that the excitation functions for multi-strange hypernuclear residues (figs. 6–8) have the same saturation-like behavior. The probability for the formation of residues with one additional captured hyperon decreases by two order of magnitude in the collisions of heavy nuclei. This difference increases up to four order of magnitude for the very light nuclei. Actually, our predicted yields of the hyper-residues may be parameterized in the wide mass range (from carbon to lead) and used for preparing the corresponding measurements. The reason of the decreasing of the hyper-residues yields for smaller colliding nuclei is just that less hyperons are produced in the collision events. Still these cross sections are sufficient for the systematic investigation of hypernuclei. Moreover, in some cases the light colliding nuclei have advantages: The background conditions are better for experimental identification of hypernuclei, and their mesonic decay channels gives a chance to use the invariant mass methods well established in hypernuclei studies [14]. In relativistic ion reactions these correlations were investigated theoretically too (Ref. [26]). Therefore, the first experiments may take place on light nuclei [16]. One can see that in the case of carbon collisions (fig. 8) at the beam energy around 2 A GeV even double light hyper-residues can be produced with the cross-section approximately $\sim$1 nanonbarn. Taking into account the high intensities of future accelerators (e.g., the planned rate is nearly 10^{12} per second for the FAIR beam [29]) it is sufficient for starting a rich hypernuclear program.

It is also instructive to understand within the transport models how the variation of the hyperon production parameters can be seen in the production of hyper-residues. In fig. 9 we show the prediction of the Λ hyperon yields by using different parametrizations inside DCM: The solid line is the standard assumption on the transition from the well-known

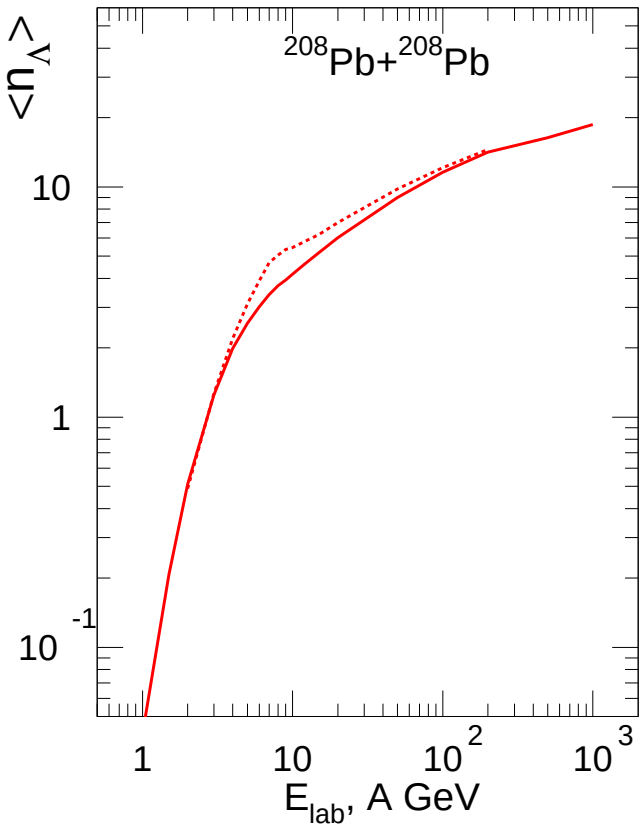

FIG. 9: (Color online) The average numbers (per event) of the Λ-hyperon production in lead on lead collisions versus the laboratory energies. The DCM calculations are integrated over all impact parameters and are performed under the standard assumption on the smooth transition between the low-energy to high-energy elementary hadron interactions (solid line), and by assuming that the employed low-energy cross-section parametrizations can also be applied at the energies which are higher approximately by two GeV (dashed line).

low-energy regime to the high energy elementary interactions described within the QGSM [40]. The dashed line presents another procedure for fitting these two limits. We note that up to now there are no sufficient experimental data available for comparison to make unambiguous conclusion about the correct excitation function of the hyperons. A small variation of the Λ yields at the energies slightly below 10 A GeV may result in a specific feature of the hyper-residue yields: We see from Fig. 10 that if we involve an alternative DCM parametrization, leading to the dashed line in Fig. 9, one can get even local maxima

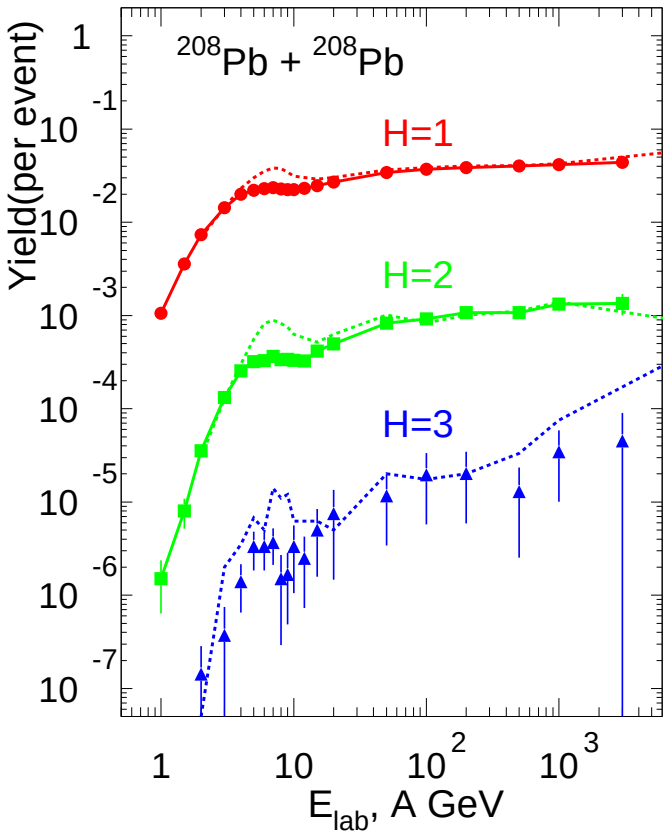

FIG. 10: (Color online) Relative yields (per one inelastic event) of the hyper-spectator residues (projectiles or targets) in lead on lead collisions versus the laboratory energies. Solid lines and symbols are the DCM standard calculations. Dashed lines are the calculations with an alternative assumption for the Λ-hyperon formation shown by the dashed line in Fig. 9. Other notations are as in Fig. 6.

of these yields at the corresponding energies. This is a consequence of that the secondary interactions, as well as the hyperon capture in the potential well, are very sensitive to the details of the hyperon origin and energy. Such kind of behaviour of the excitation functions could be a very instructive experimental signature complementary to measuring high-energy spectra of strange particles. It may compensate partly the lack of the low-energy kaon data, since predominantly low-energy hyperons can be absorbed inside nuclei.

For the following description of the reaction processes it is important to have information about the properties of the spectator hyper-residues. Since the masses and excitation

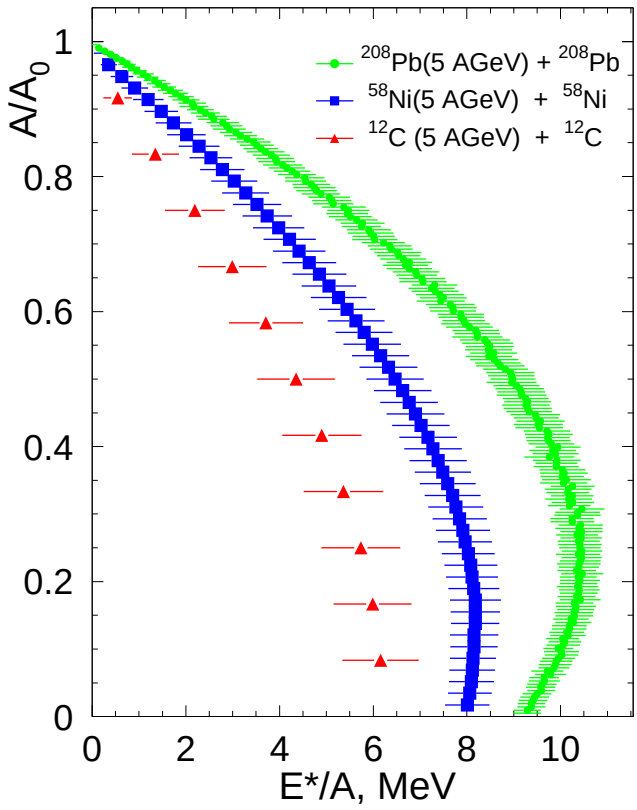

FIG. 11: (Color online) The average mass numbers of the produced residues, divided by mass number of the corresponding target and projectile, versus their excitation energy per nucleon. The 'error bars' by the symbols give the standard deviations of the DCM calculations. Reactions and laboratory energy of collision nuclei are indicated in the figure by symbols.

energies of nuclei in such intermediate states serve as input for the statistical de-excitation models. This problem was under intensive studies in relativistic heavy-ion collisions leading to the normal nuclear fragmentation. For example, as was experimentally established, there is a special correlation between a residue masses and the excitations [19, 20, 22, 54] which results in an universal fragmentation picture. The hyper-residue masses have been demonstrated in our previous works, see, e.g., fig. 7 in Ref. [25] and fig. 2 in Ref. [27]: They range from the small mass numbers to the ones close to the target and projectile. This allows for investigating a very broad distribution of hypernuclei (in mass and isospin) in the same collisions. The connection between masses and excitations obtained in the DCM

calculations, for the first time, is shown in Fig. 11. One can see that by increasing the collision violence the more nucleons are lost and the more excitation energy is deposited per nucleons. However, there is a saturation trend for the excitation, so the excitation energies which exceed essentially the nuclear binding energies are not realized in thermalized residues. We have checked that in our calculations this trend is fully consistent with the previous analysis of experimental data and it remains valid for collisions in the wide range of relativistic energies available at GSI/FAIR and other accelerators. Actually, such excited residual nuclei will decay in the fast multifragmentation/break-up and/or sequential evaporation/fission processes leading to cold hyper- and normal nuclei [19, 23, 26]. In the case of such de-excitation the captured hyperons will be predominantly concentrated in the biggest final fragments because of the considerable hyperon binding energy, see Ref. [7].

As the last step, for identification of hypernuclei, the correlation measurements (of pions, baryons and fragments) are the most promising tool for future research in this field [9, 10, 14, 26, 37, 38]. Besides identifying hypermatter, the correlations can reveal the hypernuclei properties. For example, by detecting the momenta of the decay products one can find the life-time of the hypernuclei and their binding energies. By analyzing the decay of free Λ hyperons and hypernuclei in the same events one can investigate the unbound hyperon states in double hypernuclei. It is crucial for constraining the hyperon interaction in matter and determining the properties of hypermatter at low temperatures.

V. CONCLUSION

We conclude that the spectator region in relativistic collisions of hadron and ion with ions can be a very promising source of hyper-fragments. We point that the general mechanism of such reactions leading to fragmentation and multifragmentation is well established for normal nuclear processes. Hyperons are also participating in such a process because the hyperon-nucleon interaction is of the same order as the nucleon-nucleon one. The primary produced hypermatter is relatively cold (the expected temperature of the spectator residues is not higher than T$\sim$5–7 MeV), therefore, large hypernuclei can be produced in comparison with the central collisions. A great variety of hypernuclei of all masses and in a wide range of isospin can be formed, that is similar to the phenomena existing in normal nuclei. Systematic investigations of strange and, especially, multi-strange hypernuclei can

be naturally performed in these reactions. We have demonstrated the quantitative estimates for the yields of such primary hyperfragments. The calculations are partly confirmed by a rather good description of experimental data available on the strangeness production. We have also investigated the theoretical uncertainties of the predictions by considering the variations of the model parameters, and different transport models. As we have found these uncertainties can be related to the treatment of the strange particle interaction in medium at low energy, and this opens an complementary way for experimental investigation of such processes. From the current experiments we know that the values of the hypernuclei yields obtained within our approach are sufficient for the systematic experimental measurements. Moreover, our predictions of the yields can be naturally extended for the whole mass and energy range available for targets/projectiles in future experiments. The saturation of the hypernuclei production at high laboratory energies indicate that high intensities of the accelerators and a more sophisticated detection technique are more important for this purpose than the ultra-high colliding energies.

In this respect it is encouraging that the residues of ions and their decay products with energies from 1–2 A GeV (i.e., around the hypernuclear threshold) and up to 10–15 A GeV can be effectively studied with the modern experimental installations, like FRS/Super-FRS and CBM at GSI and FAIR. These experiments are in preparation. New exotic hypernuclei can be investigated in such reactions, and new methods of their determination (e.g., by using many-particle correlations) can be applied, which may give advantages over the traditional hypernuclear studies.

Acknowledgments

A.S.B. acknowledges the support of BMBF. Also we acknowledge a partial support of GSI and the Research Infrastructure Integrating Activity Study of Strongly Interacting Matter HadronPhysics3 under the 7th Framework Programme of EU (SPHERE network). A.S.B. and K.K.G. thank the Frankfurt Institute for Advanced Studies J.W. Goethe University for hospitality.

---

[1] H. Bando, T. Mottle, and J. Zofka, Int. J. Mod. Phys. **A5**, 4021 (1990).

[2] J. Schaffner, C.B. Dover, A. Gal, C. Greiner, and H. Stoecker, Phys. Rev. Lett. **71**, 1328 (1993).

[3] W. Greiner, J. Mod. Phys. **E5**, 1 (1996).

[4] O. Hashimoto, H. Tamura, Prog. Part. Nucl. Phys. **57**, 564 (2006).

[5] J. Schaffner-Bielich, Nucl. Phys. A **804**, 309 (2008).

[6] Special issue on *Progress in Strangeness Nuclear Physics*, Edt. A. Gal, O Hashimoto and J. Pochodzalla, Nucl. Phys. A **881**, 1-338 (2012).

[7] N. Buyukcizmeci, A.S. Botvina, J. Pochodzalla, and M. Bleicher, Phys. Rev. C **88**, 014611 (2013).

[8] T. Hell and W. Weise, Phys. Rev. C **90**, 045801 (2014).

[9] The STAR collaboration, Science **328**, 58 (2010).

[10] B. Dönigus *et al.* (ALICE collaboration), Nucl. Phys. A**904-905**, 547c (2013).

[11] The PANDA collaboration, http://www-panda.gsi.de ; and arXiv:physics/0701090.

[12] G. Agakishiev *et al.*, arXiv:1310.6198 (2013).

[13] I. Vassiliev for CBM collaboration. Hypernuclei program at the CBM experiment. HYP2015, http://indico2.riken.jp/indico/contributionListDisplay.py?confId=2002

[14] T.R. Saito *et al.* (HypHI collaboration), Nucl. Phys. A **881**, 218 (2012); C. Rappold *et al.*, Phys. Rev. C **88**, 041001 (R) (2013).

[15] https://indico.gsi.de/event/superfrs3 (access to pdf files via timetable and key 'walldorf').

[16] C.Rappold, T.R. Saito, and C. Scheidenberger. Simulation Study of the Production of Exotic Hypernuclei at the Super-FRS (at GSI Scientific report 2012), GSI Report 2013-1, 176 p. (2013). http://repository.gsi.de/record/52079 .

[17] NICA White Paper, http://theor.jinr.ru/twiki-cgi/view/NICA/WebHome ; http://nica.jinr.ru/files/BM@N .

[18] M. Danysz and J. Pniewski, Philos. Mag. **44**, 348 (1953).

[19] J.P. Bondorf, A.S. Botvina, A.S. Iljinov, I.N. Mishustin, and K. Sneppen, Phys. Rep. **257**, 133 (1995).

[20] H. Xi *et al.*, Z. Phys. A **359**, 397 (1997).

[21] R.P. Scharenberg *et al.*, Phys. Rev. C **64**, 054602 (2001).

[22] R. Ogul *et al.*, Phys. Rev. C **83**, 024608 (2011).

[23] A.S. Botvina and J. Pochodzalla, Phys. Rev. C **76**, 024909 (2007).

[24] S.Das Gupta, Nucl. Phys. A **822**, 41 (2009).

[25] A.S. Botvina, K.K. Gudima, J. Steinheimer, M. Bleicher, I.N. Mishustin, Phys. Rev. C **84**, 064904 (2011).

[26] A.S. Botvina, K.K. Gudima, J. Pochodzalla, Phys. Rev. C **88**, 054605 (2013).

[27] A.S. Botvina *et al.*, Phys. Lett. B **742**, 7 (2015).

[28] Th. Aumann, Progr. Part. Nucl. Phys. **59**, 3 (2007).

[29] H. Geissel *et al.*, Nucl. Inst. Meth. Phys. Res. B **204**, 71 (2003).

[30] Y.-G. Ma (for STAR/RHIC collaboration), talk at NUFRA2013 conference, Kemer, Turkey, 2013, http://fias.uni-frankfurt.de/historical/nufra2013/.

[31] P. Camerini (for ALICE/LHC collaboration), talk at NUFRA2013 conference, Kemer, Turkey, 2013, http://fias.uni-frankfurt.de/historical/nufra2013/.

[32] A. Andronic, P. Braun-Munzinger, J. Stachel, H. Stöcker, Phys.Lett. B **697**, 203 (2011).

[33] J. Steinheimer, K. Gudima, A. Botvina, I. Mishustin, M. Bleicher, H. Stöcker, Phys. Lett. B **714**, 85 (2012).

[34] M. Wakai, H. Bando and M. Sano, Phys. Rev. C **38**, 748 (1988).

[35] Z.Rudy, W.Cassing *et al.*, Z. Phys. A **351**, 217 (1995).

[36] Th. Gaitanos, H. Lenske, and U. Mosel, Phys. Lett. B **675**, 297 (2009).

[37] T.A. Armstrong *et al.*, Phys. Rev. C **47**, 1957 (1993).

[38] H. Ohm *et al.*, Phys. Rev. C **55**, 3062 (1997).

[39] J. Pochodzalla, Prog. Part. Nucl. Phys. **39**, 443 (1997).

[40] V.D. Toneev, N.S. Amelin, K.K. Gudima, S.Yu. Sivoklokov, Nucl. Phys. A **519**, 463c (1990).

[41] S.A. Bass *et al.*, Prog. Part. Nucl. Phys. **41**, 225 (1998).

[42] M. Bleicher *et al.*, J. Phys. G **25**, 1859 (1999).

[43] W. Cassing and E.L. Bratkovskaya, Phys. Rev. C **78**, 034919 (2008).

[44] A.S. Lorente, A.S. Botvina, and J. Pochodzalla, Phys. Lett. B **697**, 222 (2011).

[45] E.L. Bratkovskaya *et al.*, Phys. Rev. C **69**, 054907 (2004).

[46] C. Hartnack *et al.*, Phys. Rep. **510**, 119 (2012).

[47] C. Fuchs *et al.*, Phys. Rev. Lett. **86**, 1974 (2001).

[48] X. Lopez (for FOPI collaboration), Prog. Part. Nucl. Phys. **53**, 149 (2004).

[49] C. Sturm *et al.*, Phys. Rev. Lett. **86**, 39 (2001).

[50] A. Förster *et al.*, Phys. Rev. C **75**, 024906 (2007).

[51] W. Scheinast *et al.*, Phys. Rev. Lett. **96**, 072301 (2006).

[52] T. Gaitanos and H. Lenske, Phys. Lett. B **737**, 256 (2014).

[53] A. Le Fevre *et al.*, J. Phys. Conf. Ser. **668**, 012021 (2016).

[54] H. Imal *et al.*, Phys. Rev. C **91**, 034605 (2015).